ELSEVIER

Polymer 42 (2001) 9657–9663

polymer

www.elsevier.com/locate/polymer

Lyotropic liquid crystalline cellulose derivatives in blends and molecular composites

J.M.G. Cowie*, V. Arrighi, J. Cameron, I. McEwan, I.J. McEwen

Department of Chemistry, Heriot-Watt University, Riccarton Campus, Edinburgh EH14 4AS, UK

Received 28 April 2001; received in revised form 27 June 2001; accepted 3 July 2001

Abstract

Solutions of cellulose tricarbanilate (CTC) in methyl acrylate (MA) and methyl methacrylate (MMA) were prepared. The MA and MMA monomers were subsequently polymerised to produce a series of molecular composites, in which the amount of CTC and the degree of substitution (DS) of the tricarbanilate groups were varied. The CTC solutions were studied using polarised microscopy and indicated isotropic behaviour in solutions with a CTC concentration of less than 33 wt%. Solutions of 33–45 wt% CTC were found to have a nematic texture and a chiral nematic texture was detected on shearing of 45 wt% solutions. The mechanical properties and morphologies of the composites were investigated using dynamic mechanical thermal analysis (DMTA), tensile testing and scanning electron microscopy. Tensile testing measurements illustrated the reinforcing behaviour of the CTC on the composite, with the initial modulus increasing by up to 250% at 45 wt% CTC. Scanning electron microscope (SEM) micrographs for composites with <45 wt% CTC revealed a one-phase system. DMTA measurements indicated the existence of a double T_g at DS of the tricarbanilate of less than 3, with a single T_g for composites containing cellulose with degrees of carbanilate substitution equal to 3. The 45 wt% CTC composite showed a broad relaxation process at 350 K and another relaxation at higher temperature (490 K) corresponding to the glass transition of the CTC itself. This result, which is indicative of phase separation, is consistent with the SEM micrographs showing distinctive layered structures within the film.

Keywords: Molecular composite; Cellulose tricarbanilate; Methyl acrylate

1. Introduction

Molecular composites have been defined by Helminiak et al. [1,2] as miscible blends of rigid-rod and flexible-coil polymers where the rigid reinforcing component is dispersed at the molecular level in the flexible-coil matrix. These materials present several advantages over conventional fibre reinforced composites due to the absence of the fibre–matrix interface. However, as proposed originally by Flory et al. [3,4], the major drawback to preparing true molecular composites lies in the inherent immiscibility between rigid-rod and flexible-coil macromolecules.

Many rigid or semi-rigid main chain polymers form liquid crystalline phases either in solution (lyotropic) or in a given temperature range (thermotropic) and many studies have been devoted to the use of liquid crystalline polymers (LCPs) as the reinforcing component in blends [5]. The molecular orientation in the LCP tends to enhance the mechanical strength and improve thermal and mechanical resistance of the blends, but usually a multiphase rather than a single-phase system is obtained. This phase separation can be overcome if the orientation of the rigid-rod polymer can be 'locked in' by in situ polymerisation of a polymerisable solvent, i.e. a monomer [6–11].

Cellulose is a poly(1,4-β-D-glucosan) with a persistence length generally around 10 nm, which characterises it as a semi-rigid polymer [12]. While naturally occurring cellulose materials are difficult to dissolve, an extensive range of derivatives, which are soluble in organic solvents, can be prepared by substitution of the hydroxyl groups. Many cellulose derivatives form both lyotropic and thermotropic liquid crystalline phases [13], particularly cholesteric mesophases. As cellulose is a naturally occurring, renewable and biodegradable polymer, composites prepared from cellulose derivative/synthetic monomer with good mechanical properties are of enormous potential interest.

In this study, we focus on the properties of composites prepared from isotropic and anisotropic solutions of cellulose tricarbanilate (CTC) with methyl acrylate (MA) and methyl methacrylate (MMA) by in situ photopolymerisation of the

* Corresponding author. Tel.: +44-131-451-3160; fax: +44-131-451-3180.

E-mail address: j.m.g.cowie@hw.ac.uk (J.M.G. Cowie).

0032-3861/01/$ - see front matter
PII: S0032-3861(01)00483-9

MA and MMA monomer. Although the preparation, morphology and optical properties of similar composites have been already reported [14], studies of the mechanical behaviour of these materials are limited [15]. In addition, the relationship between mechanical properties and structure/morphology is still poorly understood and we therefore attempt to provide a link between dynamic mechanical thermal analysis (DMTA) data and scanning electron microscopy (SEM) analysis.

2. Experimental

2.1. Materials

CTC samples with varying degrees of substitution (DS) were produced using the following heterogeneous method. Dry cellulose powder (30 mmol) (Aldrich Chemical Co.) was soaked in distilled pyridine (250 ml) for 2 h under a nitrogen atmosphere. Phenylisocyanate (270 mmol) was then added dropwise and the mixture was refluxed at 110°C. In order to obtain different DS values, the reaction was carried out over different durations from 2 to 14 h. A clear brown viscous solution was produced, and this was concentrated and precipitated into methanol. Purification of the CTC by four re-precipitations from acetone solution into methanol and a final precipitation from ethyl acetate into methanol produced a white fibrous powder. The powder was dried in vacuo at 60°C overnight and then submitted for elemental analysis.

2.2. Elemental analysis

Cellulose derivatives were analysed for elemental composition using a Control Equipment Corp. 440 Elemental Analyser. The DS was derived by comparing experimental values of elemental analysis results with theoretical values of elemental composition, determined over the full DS range (0–3). In all cases, the DS was determined from the percentage of nitrogen as nitrogen had the largest change in percentage composition over the DS range. The five CTC samples prepared were found to have DS values of 3.0, 2.9, 2.8, 2.7 and 2.3.

2.3. Composite preparation

A range of solutions was prepared from 0 to 45 wt% CTC (DS 3.0 and 2.7) in MA and 20 wt% CTC DS 3.0, 2.9, 2.8, 2.7 and 2.3 in MA and MMA. All solutions had 0.1% photoinitiator added (Daro Cur 1173, Ciba Speciality Chemicals) and were left to homogenise for two weeks at room temperature in the dark. The viscous solutions were spread quickly into a custom built cell and polymerised under a UV lamp (3400 $\mu W/cm^3$ at 360 nm) for 30 min. The films (approximately 1 mm thick) were left for a further 30 min before drying overnight in vacuo at 60°C.

2.4. Measurements

The CTC/MA solutions were analysed using an Olympus BH-2 Polarising Optical Microscope fitted with a Linkam 'PR 600' hot stage at a heating rate of 10°C/min. Clearing temperatures were determined by observing the disappearance of the birefringent textures, while heating the samples on the microscope hotstage.

Circular dichroism analysis was carried out at room temperature on a Jasco 600 Photomultiplier, scanning within a range of 290–960 nm.

Dynamic mechanical analysis (DMA) was carried out using a TA instruments, DMA2980 dynamic mechanical analyser. The samples were run on a single cantilever flexure mode operating at an oscillating frequency of 1 Hz and a heating rate of 5°C min^{-1}. Sample size was approximately 14 mm wide, 30 mm long and 1 mm thick. Tan δ was recorded in the temperature range from 150 to 495 K.

Topographical analysis of freeze fractured film surfaces was carried out using a Hitachi S-530 scanning electron microscope (SEM). The SEM samples were gold sputter coated to approximately 20 nm and imaged using an accelerating voltage of 10 kV.

Tensile measurements were carried out on a Micromat 200 tensile tester. Film dimensions were approximately 10 mm wide, 20 mm long and 0.5 mm thick. The load cell was set at 50 N and all samples were tested at 0.01 mm/s draw rate until 15% extension or breakage.

3. Results and discussion

3.1. Polymer solutions

3.1.1. Polarising microscopy

CTC dissolves readily in MA forming optically clear, anisotropic solutions above the critical concentration of 33 wt% CTC. Sanded nematic birefringent textures are observed for all the solutions with concentrations $<$33 wt% in the CTC/MA series, which appear to be homogeneous. Between 33 and 40 wt% CTC, the sanded birefringence of the solutions produced a banded texture after unidirectional mechanical shearing indicative of a nematic mesophase (Fig. 1). A cholesteric liquid crystalline phase is only produced by annealing the solution containing 45 wt% CTC at room temperature, whereas at lower CTC content, no cholesteric texture is observed. After annealing, the sanded texture changed to form a very fine polygonal birefringent pattern (Fig. 2). Jiang and Huang have observed similar textures for ethylcyanoethyl cellulose in acrylic acid [15,16], termed polygonal, they postulate that this birefringence results from the cholesteric mesophase in which the helical axes run parallel to the film surface. On cooling the 45 wt% CTC solution to below room temperature, a distinct red colour develops. This observed selective

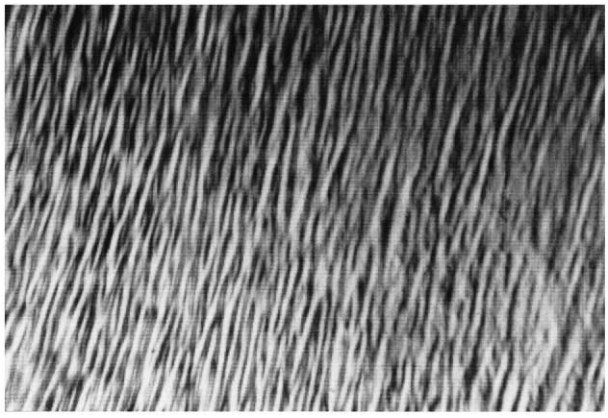

Fig. 1. Polarised optical micrograph of 40 wt% CTC in methylacrylate, obtained after shearing.

reflectance indicates that at this temperature and concentration, the solution is cholesteric in nature.

The clearing temperatures of the lyotropic solutions are shown in Table 1. As the CTC content increases, a rise in the clearing temperature is observed, indicating an increasing thermal stability of the system. At 45 wt% CTC, the onset concentration for the cholesteric phase, the clearing temperature decreases, possibly due to a mesophase to mesophase phase transition.

3.2. Composite films

3.2.1. Circular dichroism analysis

Circular dichroism was carried out, at room temperature, on the composite of 45 wt% CTC in PMA to ascertain if the cholesteric nature of the CTC was maintained within the composite after the polymerisation reaction. The spectrum produced (Fig. 3) clearly illustrates negative selective reflectance at ~620 nm in the yellow region of the visible spectrum indicating that the CTC does indeed maintain its cholesteric behaviour and has a right handed helix.

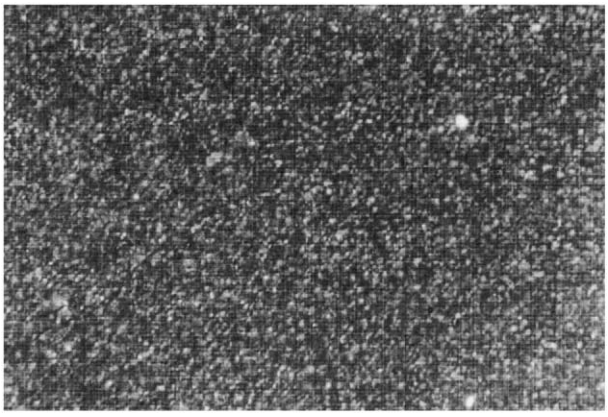

Fig. 2. Polarised optical micrograph of 45 wt% CTC in methylacrylate, obtained after annealing for 1 h at room temperature.

Table 1
Clearing temperatures of CTC/MA solutions

wt%	Appearance/optical properties	T_c (K)
33.9	Slightly viscous, clear solution/sanded texture	312.5
37.7	Slightly viscous, clear solution/sanded texture	319
39.9	Viscous, clear solution/sanded texture	323.5
41.8	Viscous, clear solution/sanded texture	334
43.4	Viscous, clear solution/sanded texture	341
45.8	Highly viscous, clear solution/ sanded texture	339

3.2.2. DMTA measurements

The CTC/poly(methyl acrylate) (PMA) composites were prepared by polymerising the MA matrix around the CTC, thus 'freezing in' the lyotropic liquid crystalline order. The translucent films exhibit increased rigidity compared to the original PMA sample with the stiffness escalating to produce a brittle composite at 45 wt% CTC.

Fig. 4 shows the variation of tan δ with temperature for composite films of 20 wt% CTC, of varying DS values, in PMA and T_g values are shown in Table 2. The T_gs for the pure components, obtained by DMTA, were 308 K for PMA and 490 K for CTC. The film that contains CTC with a DS of 3 exhibits a single glass transition in the form of a single, if broad, peak in tan δ. This is not the case when the DS is reduced. Each reduction leads to a further broadening of the glass transition region where another relaxation process is observed as a shoulder on the original T_g. This suggests that as the DS is reduced, the system becomes less homogeneous. The samples which are not fully substituted have remaining hydroxyl groups which are available for intermolecular hydrogen bonding between the CTC molecules and this could result in an element of aggregation and hence

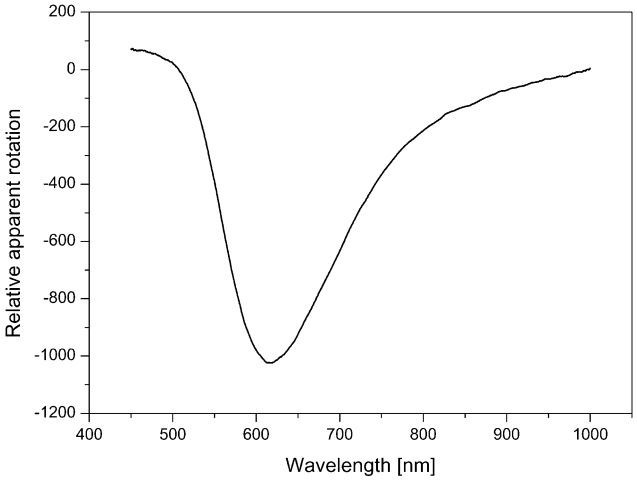

Fig. 3. Circular dichroism spectrum of 45 wt% CTC in PMA.

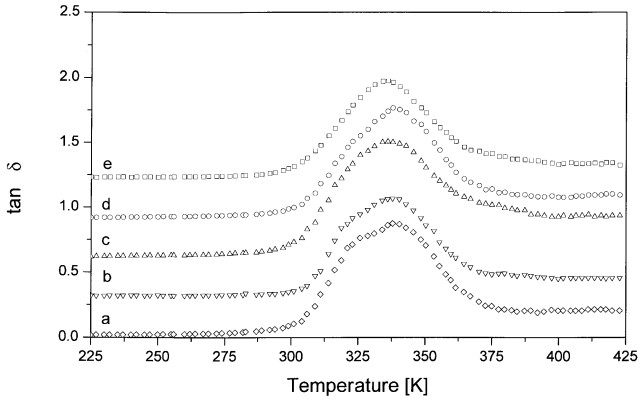

Fig. 4. Tan δ vs temperature of CTC/PMA composites: (a) 20 wt% CTC (DS 2.3), (b) 20 wt% CTC (DS 2.7), (c) 20 wt% CTC (DS 2.8), (d) 20 wt% CTC (DS 2.9), and (e) 20 wt% CTC (DS 3.0). The data have been displaced vertically by a tan δ of 0.3 for clarification.

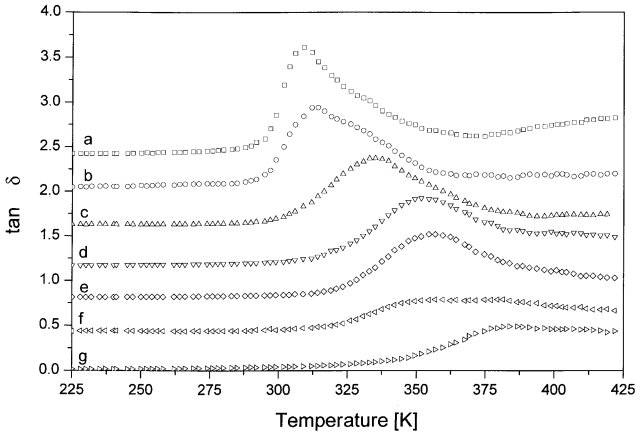

Fig. 5. Tan δ vs temperature of CTC (DS 3.0)/PMA composites: (a) 5 wt% CTC, (b) 10 wt% CTC, (c) 20 wt% CTC, (d) 30 wt% CTC, (e) 40 wt% CTC, (f) 45 wt% CTC, and (g) 50 wt% CTC. The data have been displaced vertically by a tan δ of 0.4 for clarification.

the loss of homogeneity. Alternatively, the apparent splitting of the T_g could result from the varying degrees of mobility of the PMA chains within the composites. Tsagaropoulos and Eisenberg [17] have observed similar double T_g results for several polymers containing fine silica particles. The first glass transition was identified with the normal bulk polymer T_g, whereas the second one was attributed to polymer chains with reduced mobility close to the filler surface. The existence of two T_gs could therefore be a result of heterogeneously distributed regions of different mobility with hydrogen bonded aggregates acting as pseudo-filler particles in this instance.

Fig. 5 shows the tan δ plots for the CTC (DS 3.0)/PMA composite series from 5 to 50 wt% CTC. The glass transition temperature of the pure PMA component was measured as 300 K, whereas the composite T_g values (Table 3) shift to higher temperatures with increasing CTC contents (Table 3) and the glass transition region broadens. In addition, the shape and character of the tan δ curves vary with the CTC concentration. While the tan δ curve of PMA (not shown in Fig. 5) is a single sharp relaxation, indicative of a homogeneous system, the composite tan δ peaks are much broader. A second relaxation process is observable as a shoulder above the 'original' T_g for samples with 5 and 10 wt% CTC, indicating possible inhomogeneity or lack of complete dispersion of the cellulose derivative in the matrix. Above 30 wt%, CTC a much broader, less intense, asymmetrical curve is produced and separate relaxation processes cannot be distinguished.

DMTA measurements for CTC with a DS of 2.7, over a CTC composition range of 5–45 wt% were performed and are shown in Fig. 6. The 'dominant' T_g values are shown in Table 3. These samples show a 'double' T_g in all cases, with gross phase separation occurring in the 45 wt% CTC sample, as evidenced by a distinct, second, higher temperature T_g corresponding to that of pure CTC. This was the only measurement where a relaxation process attributed to the T_g of the CTC component was detected.

In order to determine if the apparent double T_g, resulting from the DS change was unique to this system, these measurements were then repeated on the same cellulose derivatives, but now with PMMA as the polymerised matrix (Fig. 7, Table 2). Again, it is evident that for the composite with a DS of 3, there is a single well defined glass transition process. As the DS is reduced, the glass transition region broadens, confirming that there is a decrease in the homogeneity of the systems. The composites prepared with 20% CTC in PMMA softened completely some 20° above the glass transition temperature and as a result, there is a rapid rise in the tan δ curves above 425 K.

Table 2
Glass transition temperatures for CTC/PMA and CTC/PMMA composites

DS	T_g[a] (K)	T_g[b] (K)
3.0	335	399
2.9	329 & 340	396 & 410
2.8	327 & 340	394 & 410
2.7	325 & 339	395 & 412
2.3	325 & 329	397 & 416

[a] 20 wt% CTC in PMA.
[b] 20 wt% CTC in PMMA.

Table 3
Glass transition temperatures for CTC/PMA composites

CTC (DS 3.0) in PMA		CTC (DS 2.7) in PMA	
wt% CTC	T_g (K)	wt% CTC	T_g (K)
5	310	5	303
10	313	10	310
20	335	20	325
30	354	30	334
40	358	40	349
45	–	45	361

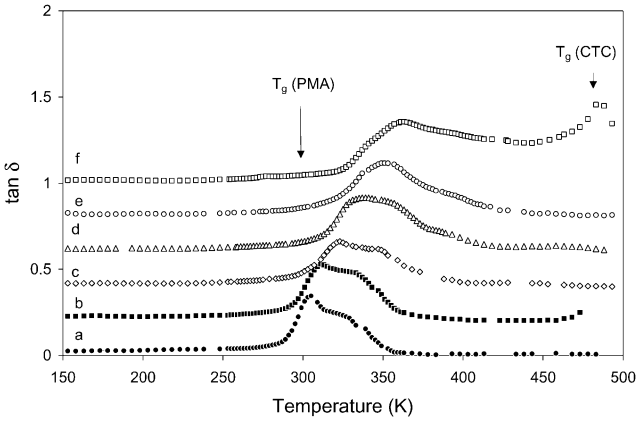

Fig. 6. Tan δ vs temperature of CTC (DS 2.7)/PMA composites: (a) 5 wt% CTC, (b) 10 wt% CTC, (c) 20 wt% CTC, (d) 30 wt% CTC, (e) 40 wt% CTC, and (f) 45 wt% CTC. The data have been displaced vertically by a tan δ of 0.2 for clarification.

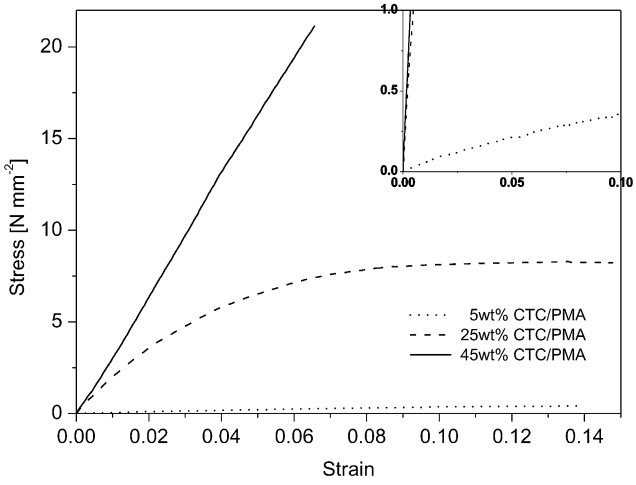

Fig. 8. Stress–strain response of 5, 25 and 45 wt% CTC/PMA films, with expanded inset (all samples were tested to break).

3.2.3. Tensile testing

The stress–strain behaviour of composites (CTC DS 2.7) was measured during tensile deformation and representative results for the 5, 25 and 45 wt% samples are shown in Fig. 8. The 5 wt% material showed an elastic response with the breaking point occurring during the plastic deformation region. The 25 wt% sample shows similar plastic character to the 5 wt% sample, but with a distinct increase in the initial elastic modulus. The 45 wt% sample exhibits a further rise in the initial elastic modulus but fractures much earlier in the elastic deformation region. This early breakage behaviour is typical of a brittle polymeric system.

Analysis of the gradient of the initial linear elastic deformation portion was used to provide values for the modulus of elasticity or initial modulus. As shown in Fig. 9, the modulus of the composites increases steadily starting with 5 wt% CTC. A maximum 250% increase in the modulus can be observed for the 45 wt% sample (the modulus increases from the value of 1.6 N mm^{-2} for pure PMA to 456 N mm^{-2} for the 45 wt% CTC/PMA sample). Even CTC concentrations as low as 15 wt% provide around 100% improvement in the stiffness of the composite. Samples with CTC concentrations >45 wt% proved to be too brittle and inhomogeneous for tensile measurements, as samples of suitable dimensions could not be prepared. Measurements were then repeated for composites with a CTC DS of 3.0 (Fig. 9). The increase in modulus for these composites was similar to those with CTC DS 2.7, with the modulus values being slightly higher. This could result from the more homogeneous nature of these films. No significant difference was detected in the modulus of pure CTC films with different DS values.

Values of the Young's modulus for an ideal molecular composite, E_m, may be calculated from the following

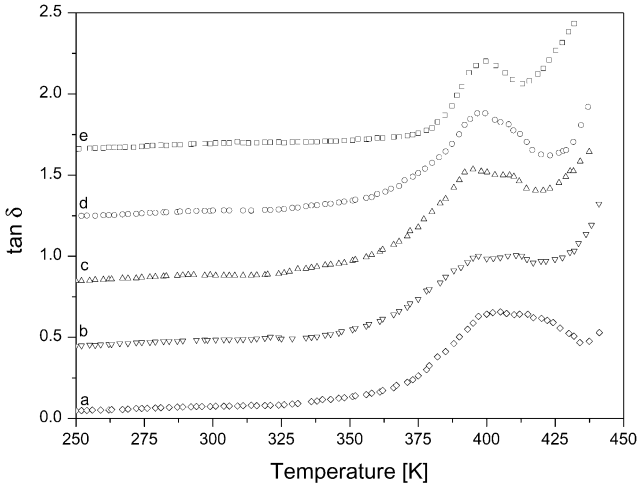

Fig. 7. Tan δ vs temperature of CTC/PMMA composites: (a) 20 wt% CTC (DS 2.3), (b) 20 wt% CTC (DS 2.7), (c) 20 wt% CTC (DS 2.8), (d) 20 wt% CTC (DS 2.9), and (e) 20 wt% CTC (DS 3.0). The data have been displaced vertically by a tan δ of 0.4 for clarification.

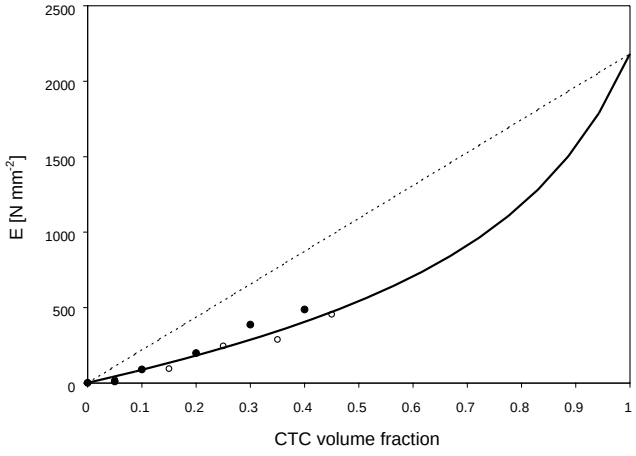

Fig. 9. Young's modulus values for CTC/PMA composites with DS 2.7 (●) and DS 3.0 (○). The experimental data are compared to calculated values using (- - -) Eq. (5) and (—) Eqs. (1)–(4) as explained in the text.

equation developed for fibres oriented randomly in three dimensions [18]:

$$E_m = \frac{1}{5}E_L + \frac{4}{5}E_T \quad (1)$$

where E_L is the longitudinal and E_T the transverse modulus, respectively. E_L can be calculated from the Halpin–Tsai equation as modified by Nielsen [18]:

$$E_L = E_r V_r + E_f V_f \quad (2)$$

where E_r and E_f are the moduli and V_r and V_f the volume fractions of the rigid and flexible components in the composite.

The transverse modulus can be determined from the semi-empirical Halpin–Tsai equation [19] which takes into account of the aspect ratio (length to diameter ratio) of the rigid, reinforcing component, ξ:

$$\frac{E_T}{E_f} = \frac{[1 + \xi B V_r}{[1 - B V_r]} \quad (3)$$

where

$$B = \frac{\left[\frac{E_r}{E_f} - 1\right]}{\left[\frac{E_r}{E_f} + \xi\right]} \quad (4)$$

As the aspect ratio, ξ, increases, E_m approaches the limiting value:

$$E_m = E_r V_r + E_f V_f \quad (5)$$

which corresponds to the Young's modulus measured in the fibre direction and calculated on the basis of the Takayanagi model [20] for a glass fibres in a plastic matrix.

Comparison of the initial moduli for films of 0–45 wt% CTC with calculated values (dashed and continuous line) is given in Fig. 9. As expected, the moduli of the composites are lower than predicted from the rule of mixtures (Eq. (5)). However, it was noted earlier that the presence of CTC causes a considerable increase in Young's modulus. Using Eqs. (1)–(4), it is possible to estimate the aspect ratio of the CTC molecules. The continuous curve in Fig. 9 was calculated using $\xi = 400$, a value which is close to that reported for composites containing rigid-rod like polymers [19].

3.2.4. SEM measurements

The morphology of the composite samples was investigated by SEM analysis. Fig. 10(a) shows a micrograph typical of the freeze-fracture surfaces from 20 to 40 wt% CTC (DS 2.7)/PMA composition region. Although these samples appeared to be slightly opaque, no phase separation can be observed in the micrographs. This result does not exclude the possibility that a certain degree of microphase separation may occur in these composites and we currently investigated this possibility using light scattering and small angle X-ray scattering. Gross phase separation is only observed for the sample in which the CTC composition reaches 45 wt%, as shown in Fig. 10(b)

This result for the 45 wt% composite is in accord with the DMTA data (Fig. 6) where a second high temperature tan δ peak corresponding to the T_g of pure CTC was observed. The phase separation process produces periodic lamellar like structures that develop throughout the film fracture surface. Some areas of the layering are reminiscent of the cholesteric fingerprint textures, which are usually observed in cholesteric liquid crystals using optical microscopy. As the CTC/MA solutions formed nematic textures, the SEM results suggest that the polymerisation process induces formation of the cholesteric ordering of the CTC in the PMA matrix. These and more extensive observations are the subject of a more detailed discussion of these composites and will appear in a future publication.

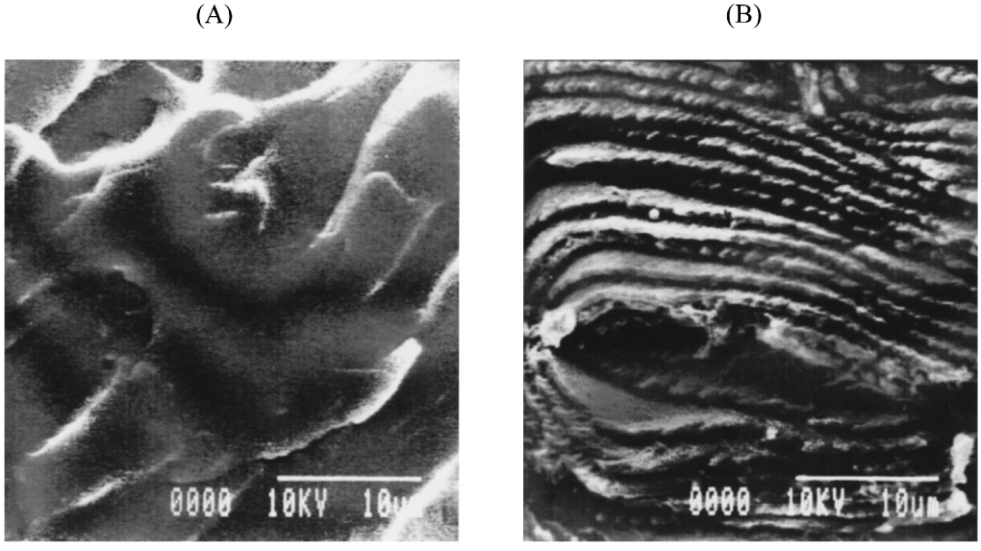

Fig. 10. SEM micrograph of (A) 20 wt% CTC (DS 2.7)/PMA composite, and (B) 45 wt% CTC (DS 2.7)/PMA composite.

4. Conclusion

CTC dissolves readily in MA and forms nematic liquid crystalline solutions above 33 wt% CTC concentration. The polymerisation of the MA around the CTC produces composites in which the PMA matrix entraps the liquid crystalline character of the CTC solutions. The morphology and structure of the composites were investigated by DMTA and SEM analysis, and the mechanical properties of CTC/PMA composites appear to be directly influenced by their internal structure. Tensile testing measurements show the reinforcing nature of the cellulose component, with the initial modulus increasing by up to 250% at 45 wt% CTC. The DMTA data indicate that microphase separation occurs in the CTC/PMA composites at all concentrations, where the DS of the CTC is less than 3. This is shown by the presence of two overlapping tan δ peaks. Composites prepared using CTC with a DS of 3 appear to be homogeneous over the concentration range of 20–40 wt%. Gross phase separation was detected only for samples containing 45 wt% CTC (DS 2.7) by both DMTA and SEM analysis.

Acknowledgements

Dr J.D. Cameron and Dr I. McEwan gratefully appreciate funding from EPSRC and acknowledge Dr D. Robson for the use of SEM facilities at Galashiels and Dr N. Price at Glasgow University for the use of CD facilities.

References

[1] Helminiak TE, Arnold FE, Benner CI. ACS Polymer Prep 1975;16:659.
[2] Helminiak TE. Div Org Coat Plast Chem Prep 1979;40:475.
[3] Abe A, Flory PJ. Macromolecules 1978;11:1122.
[4] Flory PJ. Macromolecules 1978;11:1138.
[5] Isayev AI, Kyn T, Cheng SZD. Liquid-crystalline polymer systems — technological advances. ACS Symp Ser 1996:632.
[6] Tsutsui T, Tanaka R. J Polym Sci, Polym Lett Ed 1980;18:17.
[7] Tsutsui T, Tanaka R. Polymer 1981;22:117.
[8] Nishio Y, Yamana T, Takahashi S. J Polym Sci, Phys Ed 1985;23:1043.
[9] Kozakiewicz JJ. Macromolecules 1986;19:1262.
[10] Kozakiewicz JJ. J Appl Polym Sci 1987;34:1109.
[11] Jiang SH, Huang Y. J Appl Polym Sci 1993;49:125.
[12] Gray DG. In: Shibaev VP, Lam L, editors. Liquid crystalline and mesomorphic polymers. Berlin: Springer, 1993. p. 295.
[13] Gray DG. Appl Polym Symp 1983;37:179.
[14] Müller M, Zentel R. Macromol Chem Phys 2000;201:2055.
[15] Jiang SH, Huang Y, Shen JR. J Appl Polym Sci 1995;57:493.
[16] Jaing SH, Huang Y. J Appl Polym Sci 1993;50:607.
[17] Tsagaropoulos G, Eisenberg A. Macromolecules 1995;28:6067.
[18] Nielsen LE. Mechanical properties of polymers and composites, vol. 2. New York: Marcel Dekker, 1974.
[19] Hwang W-F, Wiff DR, Benner CL, Helminiak TE. J Macromol Sci Phys 1983;B22:231.
[20] Takayanagi M. Polymeric multicomponent materials. New York: Wiley, 1997.